A human clinical trial using ultrasound and microbubbles to enhance gemcitabine treatment of inoperable pancreatic cancer

Georg Dimcevski, Spiros Kotopoulis, Tormod Bjånes, Dag Hoem, Jan Schjött, Bjørn Tore Gjertsen, Martin Biermann, Anders Molven, Halfdan Sorbye, Emmet Mccormack, et al.

Journal of Controlled Release 243 (2016) 172–181

Contents lists available at ScienceDirect

Journal of Controlled Release

journal homepage: www.elsevier.com/locate/jconrel

A human clinical trial using ultrasound and microbubbles to enhance gemcitabine treatment of inoperable pancreatic cancer☆

Georg Dimcevski [a,b,*], Spiros Kotopoulis [a,b], Tormod Bjånes [c], Dag Hoem [d], Jan Schjøtt [c,e], Bjørn Tore Gjertsen [f,g], Martin Biermann [h,b], Anders Molven [i,j], Halfdan Sorbye [k,e], Emmet McCormack [e,g], Michiel Postema [l,m], Odd Helge Gilja [a,b]

[a] National Centre for Ultrasound in Gastroenterology, Haukeland University Hospital, Bergen, Norway
[b] Department of Clinical Medicine, University of Bergen, Bergen, Norway
[c] Laboratory of Clinical Biochemistry, Section of Clinical Pharmacology, Haukeland University Hospital, Bergen, Norway
[d] Department of Surgical Sciences, Haukeland University Hospital, Norway
[e] Department of Clinical Science, University of Bergen, Bergen, Norway
[f] Centre for Cancer Biomarkers, CCBIO, Department of Clinical Science, University of Bergen, Bergen, Norway
[g] Department of Internal Medicine, Hematology Section, Haukeland University Hospital, Bergen, Norway
[h] Department of Radiology, Haukeland University Hospital, Bergen, Norway
[i] Department of Pathology, Haukeland University Hospital, Bergen, Norway
[j] Gade Laboratory for Pathology, Department of Clinical Medicine, University of Bergen, Bergen, Norway
[k] Department of Oncology, Haukeland University Hospital, Bergen, Norway
[l] Institute of Fundamental Technological Research, Polish Academy of Sciences, Warszawa, Poland
[m] School of Electrical and Information Engineering, Chamber of Mines Building, University of the Witwatersrand, Johannesburg, South Africa

ARTICLE INFO

Article history:
Received 2 July 2016
Received in revised form 7 October 2016
Accepted 10 October 2016
Available online 12 October 2016

Keywords:
Ultrasound
Microbubbles
Sonoporation
Pancreatic cancer
Image-guided therapy
Clinical trial

ABSTRACT

Background: The primary aim of our study was to evaluate the safety and potential toxicity of gemcitabine combined with microbubbles under sonication in inoperable pancreatic cancer patients. The secondary aim was to evaluate a novel image-guided microbubble-based therapy, based on commercially available technology, towards improving chemotherapeutic efficacy, preserving patient performance status, and prolonging survival.
Methods: Ten patients were enrolled and treated in this Phase I clinical trial. Gemcitabine was infused intravenously over 30 min. Subsequently, patients were treated using a commercial clinical ultrasound scanner for 31.5 min. SonoVue® was injected intravenously (0.5 ml followed by 5 ml saline every 3.5 min) during the ultrasound treatment with the aim of inducing sonoporation, thus enhancing therapeutic efficacy.
Results: The combined therapeutic regimen did not induce any additional toxicity or increased frequency of side effects when compared to gemcitabine chemotherapy alone (historical controls). Combination treated patients ($n = 10$) tolerated an increased number of gemcitabine cycles compared with historical controls ($n = 63$ patients; average of 8.3 ± 6.0 cycles, *versus* 13.8 ± 5.6 cycles, $p = 0.008$, unpaired t-test). In five patients, the maximum tumour diameter was decreased from the first to last treatment. The median survival in our patients ($n = 10$) was also increased from 8.9 months to 17.6 months ($p = 0.011$).
Conclusions: It is possible to combine ultrasound, microbubbles, and chemotherapy in a clinical setting using commercially available equipment with no additional toxicities. This combined treatment may improve the clinical efficacy of gemcitabine, prolong the quality of life, and extend survival in patients with pancreatic ductal adenocarcinoma.

1. Introduction

A diagnosis of pancreatic ductal adenocarcinoma (PDAC) carries one of the most dismal prognoses in all of medicine. Currently the 4th most lethal cancer in the western world, it has an average 5-year survival of approximately 5% and is predicted within the decade to become the second greatest cause of cancer death [1]. Surgery provides the only possibility for cure, however >85% of newly diagnosed pancreatic tumours are considered unresectable due to locally advanced disease with encasement of large blood vessels or metastasis. Furthermore, the prevalence of extreme desmoplasia generally renders the disease resistant to chemo-radiative approaches [2]. Untreated, locally advanced PDAC patients have a median survival of 6–10 months and 3–5 months for

☆ ClinicalTrials.gov number: NCT01674556

* Corresponding author at: Department of Medicine, Haukeland University Hospital, 5021 Bergen, Norway.
E-mail address: Georg.dimcevski@helse-bergen.no (G. Dimcevski).

http://dx.doi.org/10.1016/j.jconrel.2016.10.007

patients with metastatic disease [3–5] highlighting the immediate and dire need for novel therapeutic interventions.

Gemcitabine has been the standard chemotherapeutic used in recent years and the most effective single agent. Compared to 5-fluorouracil, gemcitabine extends the survival by approximately one month whilst also improving clinical symptoms [6]. Recently, FOLFIRINOX (bolus and infusion of 5-fluorouracil, leucovorin, irinotecan, and oxaliplatin) emerged as a new chemotherapeutic option for patients with metastatic pancreatic cancer and an Eastern Cooperative Oncology Group (ECOG) performance status of 0–1. For this cohort of patients FOLFIRINOX is now the reference treatment. However, owing to the demonstrable toxicities and side effects of this therapy, gemcitabine is still the standard of care in patients with poor performance status or contraindication to FOLFIRINOX [7]. Furthermore, the combination of nanoparticle albumin-bound paclitaxel (nab-paclitaxel) and gemcitabine provides another new therapeutic option resulting with improved median survival of 1.8 months, compared to gemcitabine alone [8]. Despite these novel interventions, the reported increases in survival are minimal and we continue our wait for a therapy that will impact survival, provide a bridge to reductive surgery and ultimately cure PDAC.

Diagnostic ultrasound (US) imaging has been used in the clinic for > 50 years [9,10], with detection of pancreatic lesions dating back to the late 1960s [11]. Over the past 30 years, the use of ultrasound to detect PDAC has significantly increased [11–13]. Contrast-enhanced ultrasound uses stabilised gas microbubbles (MBs) to enhance the signal-to-noise ratio of the vasculature and allows clinicians to better visualise tissue perfusion. Twenty years ago, researchers discover that upon application of ultrasound these microbubbles volumetrically oscillate. If these oscillating microbubbles were in the vicinity of cells, small pores could be formed increasing the uptake of macromolecules significantly [14–16]. Henceforth, the use of ultrasound and microbubbles to invoke biomechanical effects that increase the permeability of the vascular barrier and/or the extravasation of drug in a specific location is now commonly known as “sonoporation”.

Numerous researchers have shown *in vitro* and *in vivo* that sonoporation is a viable technique to improve drug delivery and improve therapeutic efficacy in various cell lines derived from pharyngeal [17], glioma [18], prostate [19,20], melanoma [21], and pancreatic cancer [22]. Sonoporation has also been used to open the blood brain barrier [23,24]. In general, sonoporation research is split into two camps: A) high-intensity, *i.e.*, using inertial cavitation [9,25–27] and/or taking advantage of the thermal effects [28,29], and B) low-intensity, *i.e.*, using stable cavitation [30,31] and non-thermal effects [32–34].

The use of high-intensity ultrasound without MB has previously been evaluated clinically and shown considerable success for pain therapy [35,36], ablation of breast fibroadenomas [37], opening the blood-brain barrier [38] and treatment of pancreatic adenocarcinoma [39]. Nevertheless, to our knowledge, there has been no clinical trial evaluating the efficacy of low-intensity ultrasound in combination with microbubbles to improve the chemotherapeutic efficacy in patients with PDAC.

We have previously demonstrated *in vitro* and preclinically in an orthotopic model of PDAC, enhanced treatment effects of gemcitabine with concurrent exposure to SonoVue® MB and US at low acoustic intensities [40]. Based on these preclinical results we initiated an open label phase I, single centre, safety evaluation study in PDAC patients by combining an ultrasound contrast agent and gemcitabine under sonication at clinical diagnostic conditions.

The primary objective of this study was to evaluate the safety and potential toxicity of gemcitabine combined with ultrasound contrast agent under ultrasound treatment in inoperable pancreatic cancer patients. The secondary objective was to evaluate a novel image-guided microbubble-based therapy, based on commercially available technology, towards improving chemotherapeutic efficacy, preserving patient performance status and prolonging survival.

2. Material and methods

2.1. Subjects

Over a 23-month period (January 2012–November 2013), we recruited ten consecutive voluntary patients with inoperable pancreatic cancer (ICD-10 C25.0–3) at Haukeland University Hospital. All had histologically verified, locally advanced (non-resectable Stage III) or metastatic (Stage IV) pancreatic adenocarcinoma. Needle biopsies were obtained either from the primary tumour or from a metastatic lesion. The tissue was processed in the diagnostic pathology laboratory according to standard routines (formalin-fixation, paraffin-embedment, staining with hematoxylin and eosin). The histology was evaluated by a senior pathologist with special competence in gastrointestinal pathology. Patients were ambulatory with an Eastern Cooperative Oncology Group (ECOG) performance status 0–1 (Table 1). Patients had to meet the standard criteria at our hospital for treatment with gemcitabine and no known intolerance to gemcitabine or SonoVue® (Bracco Imaging Scandinavia AB, Oslo, Norway) ultrasound contrast agent [45].

Historical data from PDAC patients undergoing equal gemcitabine treatment following the same inclusion and exclusion criteria, between 2009 and 2011 at Haukeland University Hospital, were used for comparison of treatment tolerance, safety, and overall survival. The only difference in treatment between the historical control group and our treated group was the addition of ultrasound and microbubbles following chemotherapeutic infusion. Gemcitabine was considered the standard of care for the treatment time period of the control patients and throughout this clinical study.

2.2. Chemotherapeutic and microbubble dosage

Two experienced oncologists, not participating in the study, were responsible for the chemotherapeutic treatment. The only divergence from normal administration practice was relocation to the research unit. We used the standard recommended treatment protocol of

Table 1
Clinico-pathological characteristics of all pancreatic cancer patients. There was no statistically significant difference between the sonoporation treated cohort and historical control group in age, body mass index and blood chemistry. CA19-9 was not recorded in the historical control cohort.

	Sonoporation ($n = 10$)		Control ($n = 63$)
Variables (unit)	Start of treatment	End of treatment	Start of treatment
Age (years)	58.8 (±9.8)	59.5 (±10)	64.8 (±14.0)
Gender (%) (male/female)	30/70		54/46
Body Mass Index (kg/m^2)	23.7 (±4.3)	23.9 (±5.1)	22.9 (±3.05)
ECOG performance status (%)			
0	50	10	71
1	50	80	29
2	0	10	
Histological type	Adenocarcinoma		
Stage			
Locally advanced	70	NA	55
Metastatic	30		45
Blood chemistry			
B-hemoglobin (g/dL)	13.4 (±1.5)	11.9 (±0.9)	12.6 (±1.5)
ALAT (U/L)	45.2 (±21.8)	59.7 (±42.9)	71.2 (±59.6)
LD (mg/dL)	151.4 (±27.6)	209.6 (±46.0)	177.7 (±49.4)
Bilirubin (μmol/L)	14.5 (±8.46)	7.3 (±4.0)	37.3 (±66.0)
CA 125 (U/mL)	54.1 (±39.6)	62 (±60.1)	90.0 (±100.5)
CA19-9 (U/mL)[a]	248.5 (±380.8)	117.1 (±202.9)	NA

Comments:
Obligatory lab values for chemotherapy inclusion: B-Hemoglobin >10, Neutrophils (polymorphoneuclear leukocytes) >3.5, Platelets >150, Bilirubin >75.
[a] One sonoporation treated patient exhibited abnormally high CA19-9 values at 4608 U/mL hence not included in average CA19-9 values.

gemcitabine hydrochloride (Gemzar®, Eli Lilly & Co., Indianapolis, USA) [45]. Specifically, an initial phase of intravenous gemcitabine infusion was administered at a frequency of one cycle per week for seven weeks followed by a one-week pause. Subsequent cycles of infusions were given once weekly for 3 consecutive weeks out of every 4 weeks. Treatment pauses or any dose adjustments were administered according to standard guidelines [43,45]. Chemotherapy was continued as long as the treatment was beneficial [46]. The patients were monitored according to the requirements for Phase I studies [47].

Maximum plasma concentration of gemcitabine is achieved after 30 min at which point sonoporation with Sonovue® was initiated to ensure maximal possible tumour exposures [48]. Clinically approved SonoVue® ultrasound contrast agent was used as the microbubble for sonoporation [49]. Ethical approval limited treatment to the use of a single vial of microbubbles, paralleling traditional imaging protocols. Due to the acoustic emission limitations of the clinical diagnostic scanner (*c.f.*, Section 2.4) we chose to maximise the treatment time to achieve the longest active sonoporation time (*i.e.*, time when ultrasound waves and microbubbles were present). The expected *in-vivo* life time of microbubbles was 4–5 min, hence we chose to inject boluses every 3.5 min to ensure microbubbles were present continuously throughout the whole treatment. Previous experience [50] showed that we were able to detect microbubble using non-linear ultrasound imaging using 0.5 ml boluses [51]. Due to these requirements, microbubble dosage results in 0.5 ml of SonoVue® followed by 5-ml saline every 3.5 min, immediately after the end of the intravenous infusion of gemcitabine [43]. A complete vial was used in 31.5 min. The total dose of contrast agent used throughout each treatment was within standard clinical practice [52].

2.3. Ultrasound scanner configuration

In our previous studies we determined that sonoporation had a significant therapeutic effect when using long pulse durations, specifically 40 μs pulses every 100 μs (*i.e.,* a duty cycle of 40%) [41,44]. This resulted in minimal acoustic energy deposition within FDA and IEC guidelines and maximum therapeutic efficacy [53,54]. In this clinical study, an unmodified clinical diagnostic ultrasound scanner (LOGIQ 9, GE Healthcare, Waukesha, WI) in combination with a 4C curvilinear probe (GE Healthcare) was used to apply the therapeutic ultrasound. Unfortunately, it is not possible to generate such long duty cycles with an unmodified clinical diagnostic machine, due to technical limitations. In addition, such long duty cycles would severely degrade the image resolution. Hence, we attempted to maximise the ultrasonic duty cycle emitted by the clinical machine, whilst keeping linear waves, to avoid bubble destruction and energy deposition at higher harmonics.

In order to determine the ideal settings, the machine was characterised and calibrated in a bespoke, automated, 3-axis ultrasound characterisation chamber filled with filtered, degassed, deionised water. To waterproof the probe prior to submersion, the transmission surface was covered in AQUASONIC® ultrasound transmission gel (Parker Laboratories, Fairfield, NJ), and subsequently covered using a latex ultrasound probe cover (Sheathing Technologies, Inc., Morgan Hill, CA). The probe was locked in place and a range of acoustic emission conditions were evaluated with the aim of reaching the longest duty cycle with linear waves (*i.e.*, minimum amount of harmonics) at a de-rated MI of 0.2. The ultrasound emission conditions were characterised following FDA and IEC ultrasound guidelines [53,54]. To achieve the maximum pulse repetition rate the packet size was maximized. Whilst this reduced the frame rate substantially, it resulted in increasing the pulse repetition significantly higher than possible with a frame rate increase alone. Knowing that each patient would have a different tumour depth and size, various focal and image depths were calibrated to ensure all patients were treated with identical conditions. The ultrasound scanner configuration was programmed to maximise the duty cycle, with short broadband linear pulse in order excite as many microbubbles as possible for the longest period possible. These acoustic emission conditions were considered optimal in relation to the limitations of the clinical ultrasound system emission configuration conditions. The device optimized acoustic conditions resulted in a derated MI of 0.2 (0.27 MPa peak-negative pressure), a 0.3% duty cycle with a center emission frequency of 1.9 MHz, and a spatial-peak temporal-average intensity of 0.25 mW/(cm) [2]. Specifically, the beamformed ultrasound bursts consisted of 4 cycles (2.1 μs) every 21 ms, *i.e.*, a transmission duty cycle of 1%. Following the completion of the 12 ultrasound packet transmissions, there was a transmission pause allowing for echo capture and image reconstruction resulting in an overall duty cycle of 0.3%. The center frequency of 1.9 MHz was ideal as it was close to the natural resonance of the SonoVue® microbubbles [55]. At an MI of 0.2, only stable cavitation was expected to be induced throughout treatment. These acoustic emission conditions resulted in a 1-cm thick treatment slice based on a −3 dB contour [43].

To make sure that treatment only occurred at the target, *i.e.,* the tumour, the image plane and non-linear contrast region of interest (ROI) was limited to the tumour area + 1 cm surrounding area. We avoided treating any liver or bowel area. The acoustic focal depth was placed at the centre of the tumour. The expected treatment height, based on a −3 dB contour was 3 cm above and below the acoustic focus depth.

This image-guided therapy model is based on the expectation that treatment only occurs where the ultrasound and microbubbles are present, *i.e.*, what is being imaged.

The ultrasound probe was re-calibrated every six months to ensure acoustic consistency. The exact acoustic conditions and the ultrasound field map are thoroughly described in our previous publication [43].

2.4. Transabdominal ultrasound

Routine abdominal US imaging [56] was performed during the last 10 min ($T = 20$ min) of chemotherapeutic delivery using the same LOGIQ 9 clinical diagnostic ultrasound scanner as for treatment. The ultrasound probe was attached to a ball-head mount allowing for initial free-hand scanning. Once in the optimal position for treating the tumour, with the largest diameter targeted, the ball-head mount was locked and the ultrasound probe was kept in this position till completion of the treatment [43] (*c.f.,* Fig. 1). The optimal treatment position of the 4C clinical diagnostic ultrasound probe to ensure a clear acoustic path to the tumour without any obstructions such as stomach and bowel air varied per patient. This was achieved by following established diagnostic protocols for imaging the pancreas [56,57]. In general, the probe was positioned in the epigastric region with the acoustic propagation path pointing towards the pancreatic tumour. The azimuth and elevation of the probe was adjusted to avoid any air pockets and liver tissue. The patients were allowed to lie in their most comfortable position prior to locating the tumour and locking the transducer in place. The patients were consulted if any discomfort was felt, and pressure adjustments were made if necessary. The large vasculature near the primary tumour was visualized using non-linear contrast mode in order to validate that microbubbles were being sonicated near the target tumour. Patient breathing allowed for passive scanning of the tumour, as with each breath the tumour would move through the acoustic field. The amount of passive scanning varied per patient breathing volume. Breathing based passive scanning ranged between 1 and 3 cm at the tumour level.

The total duration of combined ultrasound and microbubble treatment was 31.5 min. Fig. 1 shows the experimental setup used to combine chemotherapy, ultrasound, and microbubbles. Panel A shows the time course of each treatment cycle whilst Panel B shows a photograph of the ultrasound positioned to treat the tumour.

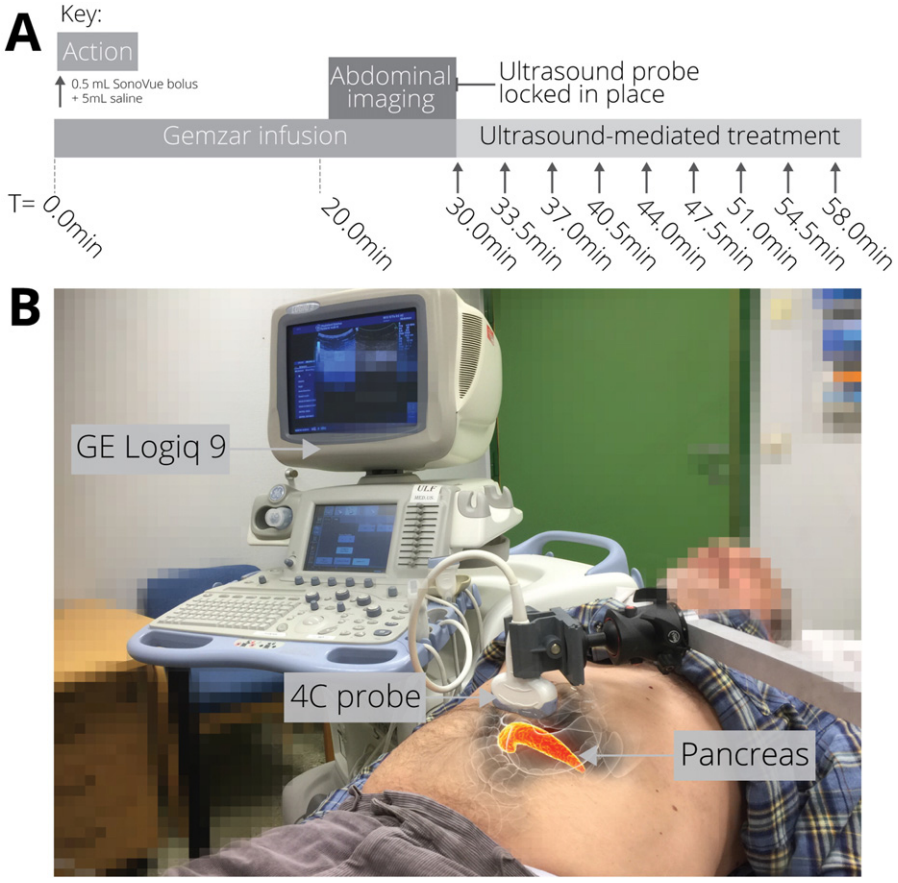

Fig. 1. (A) Treatment procedure flow chart with timings of chemotherapeutics, ultrasound exposure, and microbubble infusion. Using the current protocol, the treatment duration was 61.5 min. The first 30 min were reserved for chemotherapeutic infusion and the last 31.5 min were reserved for ultrasound and microbubble treatment. Abdominal imaging was performed for the last 10 min of infusion. Every 3.5 min, 0.5 ml of SonoVue® microbubbles were injected. (B) Photograph of patient with PDAC undergoing treatment using a clinically available diagnostic scanner. The ultrasound probe was locked in position using a mechanical arm targeted at the primary tumour for the full 31.5 min of ultrasound and microbubble treatment.

2.5. Pharmacokinetic evaluations

Analytical methods for pharmacokinetic (PK) evaluations were developed in parallel to the clinical study [58]. Whole blood samples were collected sequentially into prechilled heparinized tubes at the following time-points: $T = 0$, 30, 60, 120, 180 and 240 min. Tubes were spiked with the cytidine deaminase inhibitor tetrahydrouridine to prevent deamination of gemcitabine to dFdU [58]. Plasma and mononuclear cells were separated from whole blood as described previously. Concentrations of gemcitabine and dFdU were measured in plasma using in-house LC-MS/MS methods [58].

2.6. Monitoring

All patients underwent dual-phase computed tomography (CT) imaging ≤3 weeks before study inclusion. Routine abdominal CT was performed every 8th week where maximum tumour diameter was quantified by independent radiologists. Tumour size and development was characterised according to the Response Evaluation Criteria in Solid Tumours (RECIST). Positron emission tomography (PET) imaging with F-18-fluoro-deoxyglucose (FDG) was performed prior to the treatment to determine if metastases were present.

Assessment of clinical state during the treatment also included an evaluation of the clinical benefit response and if surgical resection could be performed [46,59]. ECOG performance status was used as a proxy to monitor the effectiveness of the combined treatment. The ECOG scale describes patients' level of functioning in terms of their ability to care for themselves, daily activity, and physical ability [46]. An ECOG grade of 0 indicates a patient who is fully active and able to carry on all pre-disease performance without restriction. An ECOG grade of 1 indicates that a patient is restricted in physical strenuous activity but ambulatory and able to carry out work of a light or sedentary nature, *e.g.,* light house work, office work. An ECOG grade of 2 indicates a patient is ambulatory and capable of all self-care but unable to carry out any work activities. The patient is up and about >50% of waking hours. An ECOG grade of 3 indicates a patient capable of limited self-care and confided to bed or chair >50% of waking hours. Hence, the longer a patient stayed below an ECOG grade of 3, the more effective the treatment was considered indicating an extended period of well-being. When a patient reaches an ECOG grade of 3, they are no-longer able to undergo gemcitabine chemotherapy.

Select patients also underwent diagnostic contrast-enhanced ultrasound following established clinical procedures [60]. Blood analysis was performed to evaluate if there was any acute toxicity.

2.7. Statistical analysis

The results are expressed as mean values ± SD, unless otherwise indicated. Continuous data was analysed using *t*-tests, or Mann-Whitney tests if data were not normally distributed. Gehan-Breslow-Wilcoxon test and Log-rank (Mantel-Cox) test were used to compare survival. Variance is expressed through 95% confidence intervals. $p < 0.05$ was considered statistical significant. Patients removed from the study due to improvement were considered as intention to treat in the survival statistical analysis.

3. Results

3.1. Tumour targeting

The established guidelines for imaging the pancreas [56,57] allowed us to target the primary PDAC tumour, independent of tumour depth and size. Fig. 2 shows four representative ultrasound images of the PDAC tumours from our treated patient cohort captured prior to switching the diagnostic ultrasound scanner settings to "treatment mode". In these images tumour depths ranges from 3.1 cm to 8.9 cm indicating that shallow or deep tumour did not inhibit tumour visualisation or targeting.

3.2. Toxicity evaluation

The direct parameters used to evaluate the toxicity of our treatment were clinical parameters including vital signs, ECG and blood chemistry. Overall, all data indicated that gemcitabine in combination with US did not induce any unexpected deviation or additional toxicities than chemotherapy alone.

One patient was hospitalised for a serious adverse event (SAE) unrelated to protocol therapy. Four SAEs occurred during protocol therapy. Two patients had symptoms indicating biliary obstruction and necessitated hospitalisation and rescheduling of the treatment. One was treated for pneumonia and one had fever due to cholangitis. The most frequent possibly treatment-related toxicities *i.e.,* adverse events (AE) were abdominal pain ($n = 9$), nausea ($n = 7$), fever ($n = 6$), neutropenia ($n = 6$), and fatigue ($n = 6$) as described in Fig. 3. These events were registered as possibly related to protocol therapy. Since all the reported toxicities are expected side effects of gemcitabine, they were evaluated as gemcitabine related. All other AE were probably related to progression of underlying disease. There were no treatment-related deaths.

3.3. Blood biochemistry

No additional toxicity was observed. Blood values changed as expected. CA 19-9 and CA 125 levels decreased in 5 out of 8 patients measured, and 7 of the 10 patients, respectively.

When evaluating the levels of cancer marker CA 125 we observed a decline following combined treatment. A total of four out of ten patients went from elevated to normal counts and only a single patient went from normal to elevated counts. Whilst fewer measurements were made in the CA 19-9 counts a similar trend was also observed where three patients went from elevated counts to normal counts, five patients showed a decrease, two patients showed an increase, and only a single patient went from normal to elevated counts. No correlation between tumour size change and cancer marker count was observed (Supplemental Fig. 1).

Bilirubin, LD, ALAT and other liver parameters were in line with the expected variation under gemcitabine treatment. These were all considered to be normal blood biochemistry changes as expected from chemotherapy and disease course.

3.4. Clinical benefit and response assessment

The following methods were applied to evaluate the responses in the ten patients: RECIST, tumour size, ECOG grade and treatment cycles [59,61].

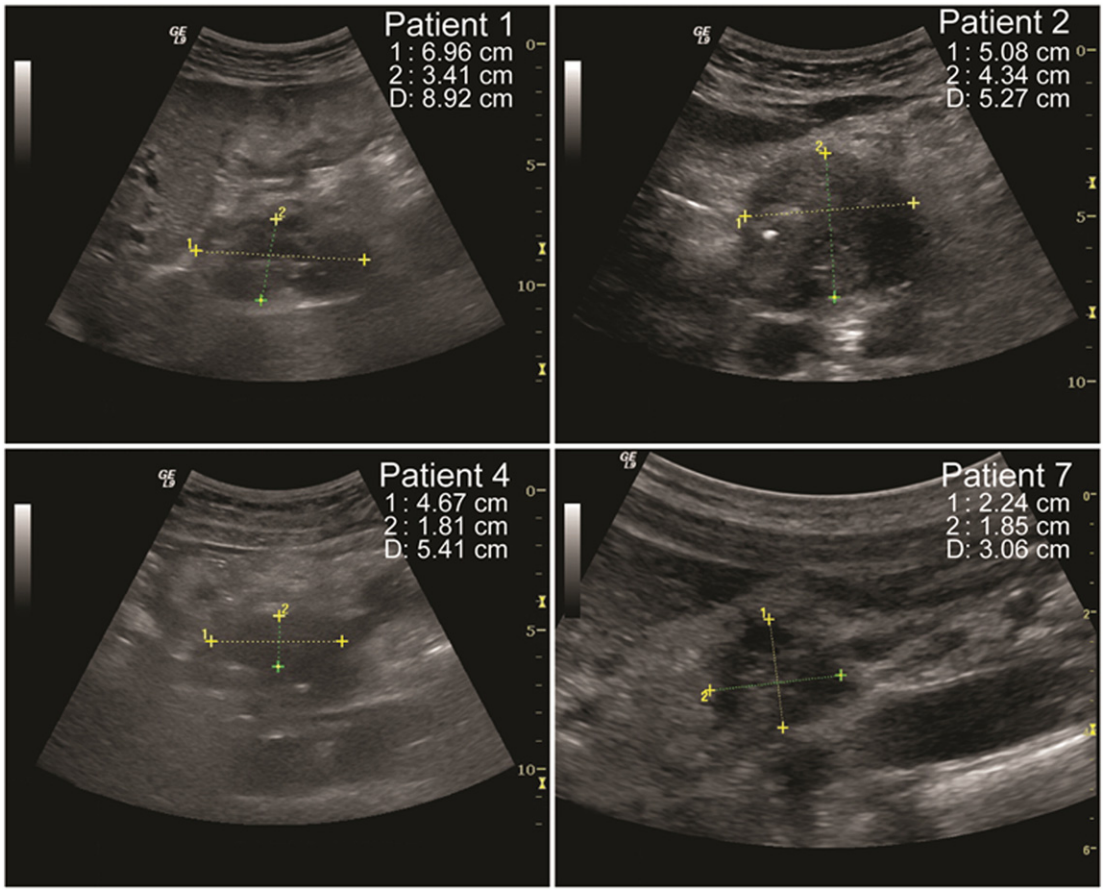

Fig. 2. Representative ultrasound images showing the PDAC tumour in four of the ultrasound and microbubble treated patients. Tumour height and width are indicated by the yellow and green dotted lines. The ultrasound transducer was positioned to ensure no obstructions of the acoustical beam path to the tumour. This resulted in a unique ultrasound probe position per patient and treatment. Distance 1 and 2 indicate the tumour width and height respectively. Value D indicated the tumour centroid depth.

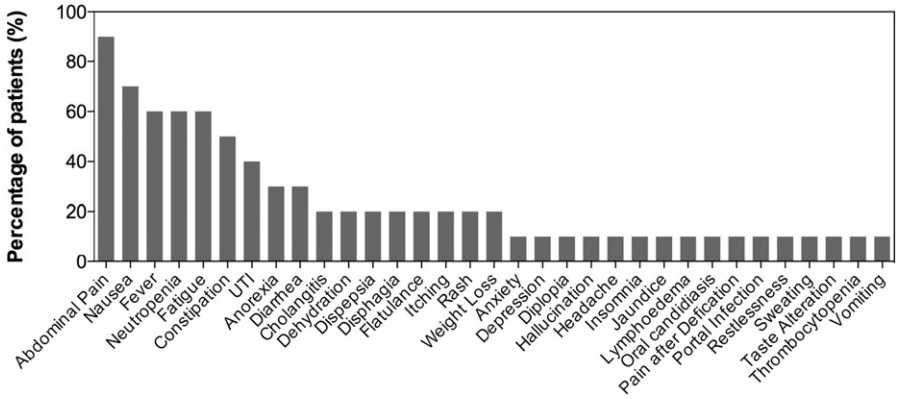

Fig. 3. Percentage of patients with PDAC treated with sonoporation that experienced a given adverse event. This graph shows all the adverse events experienced by all patients regardless of severity grade, or direct correlation to the treatment. All adverse events were already associated with gemcitabine treatment alone, indicating that addition of ultrasound and microbubbles did not induce or increase the frequency of new adverse events.

The patients considered to be positive clinical responders were regularly evaluated by the Dept. of Oncology for FOLFIRINOX treatment or consolidative radiation therapy and surgery. After 12 treatment cycles, one patient was down-staged from 8.6 cm to 4.2 cm in tumour size and thereby became available for potentially curative therapy. She was removed from the clinical trial and underwent radiation therapy and subsequent pancreatectomy. Five patients exhibited partial responses as evidenced by reduction in tumour diameter. As a result, they were offered either consolidative radiation therapy or FOLFIRINOX treatment.

Fig. 4 shows the effect of our combined treatment on the tumour size. The green lines indicate the patient tumour size recession or stabilization from the start to the end of the treatment, whereas the red lines indicate tumour size increase. When the line ends, this indicates that the patient was removed from the clinical trial.

An average of 13.8 ± 5.6 and median 12.5 (range 5–26) treatment cycles of protocol therapy were delivered per patient. In comparison, our historical control group treated with the same chemotherapeutic protocol of gemcitabine alone received an average of 8.3 ± 6.0 and median 7 (range 1–28) treatment cycles ($p = 0.008$). Fig. 5A shows a whisker plot depicting the number and range of treatment cycles.

Fig. 5B shows the survival curve of the combined treatment group compared to the historical control group. The number of treatment cycles and days of survival in our patient group are summarised in Table 2. Both Gehan-Breslow-Wilcoxon test and Log-rank (Mantel-Cox) test showed that the survival was significantly different with $p = 0.0043$ and $p = 0.011$, respectively.

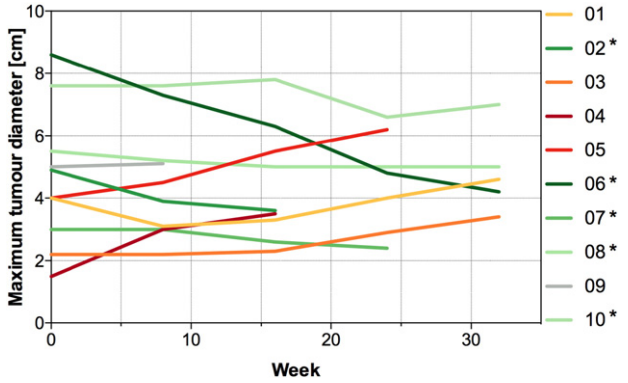

Fig. 4. Maximum tumour size as function of time for all ten patients with inoperable pancreatic adenocarcinoma. Green lines indicate tumour size recession or stabilization. Red/orange or grey lines indicate tumour size increase. Colour gradient indicates linear regression fit of tumour growth gradient (lighter = shallower). Five out of ten patients (50%) showed tumour size reduction during treatment. A reduction in tumour size may allow for surgical resection; the only current curative option. The star (*) indicates which patients showed tumour size reduction and were evaluated for consolidative radiation therapy or FOLFIRINOX treatment.

3.5. Gemcitabine pharmacokinetics

Concentration profiles of gemcitabine and dFdU in plasma samples were in accordance with previous studies of gemcitabine-infusions of 800–1000 mg/m^2 administered to breast, lung, pancreatic and patients with various other solid tumours [48,62]. This demonstrates that the combination regimen did not seem to alter the systemic pharmacokinetics of gemcitabine. A representative concentration profile from one of the patients is shown in Supplemental Fig. 2.

4. Discussion

To our knowledge, this is the first human trial evaluating the use of low intensity ultrasound and microbubbles to treat cancer. All previous studies have only been performed *in vitro* or pre-clinically. Clinical studies using ultrasound for therapy have been focused on high-intensity ultrasound without microbubbles, or for pain treatment. Hence the effect of low intensity sonoporation therapy for PDAC in humans is unknown [44,63–65].

In our previous study [43], we presented the experimental protocol focusing on the technical aspects of implementing low-intensity sonoporation using a clinical diagnostic ultrasound scanner. We also presented pilot results of five patients briefly discussing the number of cycles and tumour sizes. In the current work we present the final results and clinical data of all 10 patients, including a comparison of overall survival. In addition, we provide a toxicity report regarding the safety of the study following 138 treatment cycles.

The primary aim of this Phase I study was to evaluate the safety and potential toxicity, when combing microbubbles, ultrasound, and a chemotherapeutic agent in patients with PDAC. Hence, in this clinical trial we only evaluated a total of ten patients, as required by the NMA. Overall, all data clearly indicated that this combination did not induce any additional toxicities.

4.1. Cancer markers

These results indicate that chemotherapy in combination with microbubbles and ultrasound may have a positive impact on tumour development. It is well known that there are correlations between CA 19-9 decline and both overall survival and time to treatment failure in patients treated with gemcitabine alone [66]. The limited number of patients in our Phase-I-trial does not allow us to make any further conclusions.

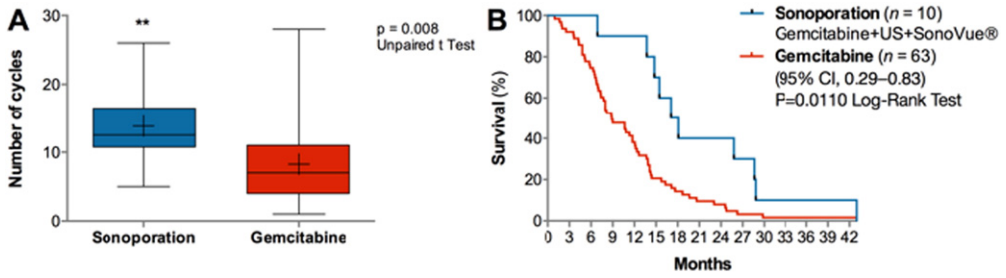

Fig. 5. (A) Whisker plot comparing the number of treatment cycles undergone in patients with pancreatic adenocarcinoma. Patients treated with sonoporation showed a statistically significant increase in number of treatment cycles ($p = 0.008$, unpaired *t*-test) indicating inhibited tumour progression and extended period of well-being (B) Survival plot comparing patients treated with ultrasound, microbubbles, and gemcitabine *vs* gemcitabine alone. The survival curve indicated that the combined treatment group had near twice as high median survival compared to treatment with gemcitabine alone; from a median of 8.9 months to 17.6 months ($p = 0.011$, Log Rank test).

4.2. Adverse events

In our present work, we present all adverse events experienced by the patients independent of grade and severity (Fig. 3). This also includes adverse events due to the actual malignancy, or personal experiences. Other clinical studies typically only register adverse events that can be directly correlated to the treatment itself, with occurrences above 10% and grades ≥ 3 [45]. As adverse events are rarely registered clinically, we were unable to directly compare with our historical group. To aid comparison we have compared to values available in literature (*c.f.*, Supplemental Fig. 3). In this Figure, we observe a 40% difference of abdominal pain. The primary symptoms of pancreatic cancer are abdominal pain and weight loss [67], as a result this symptom is rarely recorded. Nine out of our ten patients exhibited abdominal pain prior to treatment, hence we do not attribute this adverse event as treatment related. In contrast, in studies where weight loss was recorded, it was observed in nearly all patients. In our treated patient cohort, only 20% (2 patients) exhibited weight loss. Throughout this study all AE had already been previously associated with gemcitabine chemotherapy alone. This strongly suggests that there is no additional toxicity when combining ultrasound and microbubbles with gemcitabine chemotherapy.

4.3. Overall survival and well being

When the patients' health deteriorates, and their ECOG status rises above 2, they are no longer able to undergo therapy. Hence, number of treatment cycles indirectly represents the physical well-being of the patients. Our clinical trial group was able to undergo 66% more cycles than the historical control group. It is important to note that the analysis of treatment cycles is biased against the sonoporation group as four out of ten patients were removed from the study due to reduction of the tumour size. If these patients had continued treatment, the number of treatment cycles would be higher. This suggests that chemotherapy in combination with ultrasound and microbubbles may prolong the physical health and ambulatory status of patients with pancreatic cancer. Due to the study design, our data may not be directly comparable to the historical control cohort; hence these results should be interpreted with caution.

When evaluating survival, our results showed a mean survival of 21.4 months and median survival of 17.6 months. This was significantly longer than our historical control group (8.9 months) and literature values (6.7 months) [5]. Whilst these results should be interpreted carefully, we argue that chemotherapy in combination with ultrasound and microbubbles probably increases survival in patients with pancreatic cancer.

Table 2
Number of cycles and days survival as of diagnosis for patients with pancreatic cancer treated with ultrasound, microbubbles, and gemcitabine. The number of treatment cycles ranged from 5 to 26 cycles whereas survival ranged from 207 to over 1333 days.

Patient	Number of treatment cycles	Days survival
P1	26	443
P2[a]	11	207
P3	10	774
P4	16	513
P5	16	859
P6[a]	11	412
P7[a]	12	1333
P8[a]	18	543
P9	5	464
P10[a]	13	865
Average	13.8	641
Median	12.5	528
SD	5.7	322

[a] Patients removed from the study due to improvement.

4.4. Other chemotherapeutic options

Whilst gemcitabine is no longer considered at the forefront of chemotherapeutic treatment for PDAC, it was the first choice treatment when this clinical trial was initiated [68]. Other drugs and drug-combinations such as FOLFIRINOX and Gemcitabine + nab-Paclitaxel are now considered state-of-the-art [7,8]. As this trial was initiated using Gemcitabine we could not modify the protocol when other drugs and drug combinations reached the forefront of PDAC chemotherapeutic treatment. Gemcitabine is still commonly used worldwide for the treatment of PDAC, hence this protocol may allow for easier implementation.

When we compare median survivals of these patient groups from literature we see that FOLFIRINOX results in median survival of 11.7 months while gemcitabine + nab-Paclitaxel give a median survival of 12.2 months [69]. The observed median survival in our study far surpassed both these values using a less effective drug (Graphical Abstract). As sonoporation is not limited to any specific drug, inducing sonoporation with a more effective chemotherapeutic may further improve the therapeutic efficacy. In the case of combined chemotherapeutics, sonoporation could either be induced during or after infusion of all drugs, or at a time point where all chemotherapeutics are in the bloodstream.

4.5. Tumour perfusion

PDAC is well known to be a hypovascular tumour [70], meaning it has less perfusion than the tissue surrounding it. This is falsely correlated to no perfusion. Nevertheless, in the clinical field it is well known that PDAC still exhibits perfusion. An example of such hypovascular perfusion can be seen the Supplemental video 1 and Fig. 6. Fig. 6 shows a B-Mode image, contrast-enhanced image, and a perfusion curve of the aorta, healthy pancreatic tissue and the primary PDAC tumour. Microbubbles can be clearly distinguished in the primary PDAC tumour when comparing the primary PDAC tumour area in Fig. 6 A *vs.* B. The perfusion curve Fig. 6C, depicts non-linear contrast echo amplitude as

a function of time for three regions of interest (ROI). The results validate that microbubbles enter the PDAC tumour. At $T = 0$, *i.e.*, the time of injection, no microbubbles are present (*i.e*, −68 dB is the base line). At around 25 s the aorta is the first ROI to reach maximum perfusion, as expected. The pancreas reaches maximum perfusion at around 27 s, whilst the PDAC tumour reaches maximum perfusion at around 32 s. The aorta shows the highest nonlinear echo amplitude, followed by the pancreatic tissue. The PDAC has the lowest nonlinear echo amplitude whilst still being 26 dB higher than the baseline, but only 5–10 dB lower than the pancreas. This indicates the tumour has lower perfusion than the surrounding tissue, yet is sufficiently perfused to allow microbubbles to enter.

It is important to note that our historical control group treated with gemcitabine alone has a median survival of 8.9 months, which is slightly higher than that previously reported in literature (6.7 months) [3,5,71] indicating that our historical control group was not negatively biased.

4.6. Potential mechanisms of sonoporation in vivo

In vitro, sonoporation is typically evaluated on a cell monolayer allowing direct contact between the target cell line and microbubbles. *In vivo*, the microbubbles flow through the vasculature and capillaries allowing direct contact only with endothelial cells, resulting in enhanced uptake only by these cells or, in some cases, in deeper cell layers [72,73]. We believe that the therapeutic efficacy observed in this Phase I clinical trial cannot only be attributed to the potential increase of gemcitabine uptake in the endothelial cell walls. The interaction between the vascular barrier and microbubbles may result in increased fenestration size allowing deeper drug penetration [74]. It is also known that ultrasound in combination with microbubbles can increase intracellular stress signalling [75]. This increased stress, in combination with the chemotherapeutic may result in enhanced drug sensitivity. Nevertheless, further work needs to be performed, pre-clinically and clinically to ascertain the true mechanisms behind the improved therapeutic efficacy.

4.7. Limitations

Whilst all these results show great promise, we cannot make global assertions on the efficacy of ultrasound-enhanced chemotherapy based on this study. To further understand and validate these results it is paramount to perform mechanistic experimental studies and examine a larger patient cohort in a prospective randomized controlled Phase II trial.

The tumour size reduction was measured using the maximum tumour diameter. Whilst this method gives a representative overview of

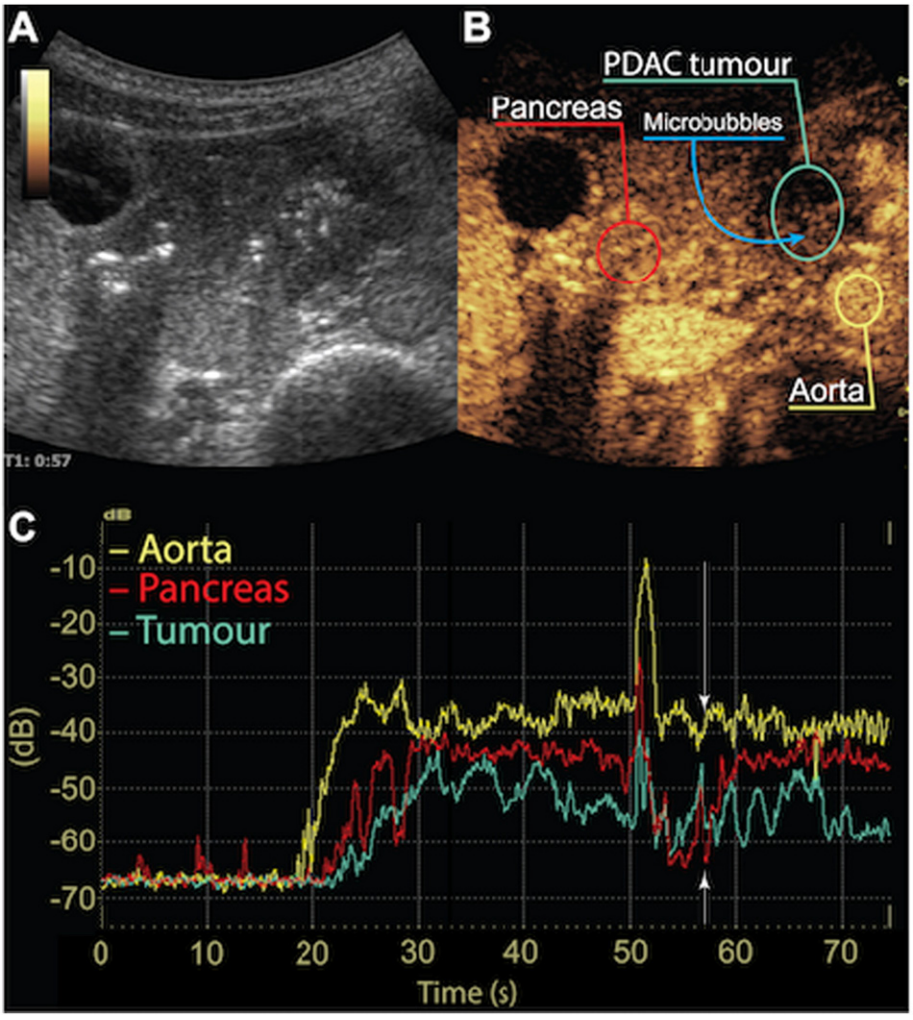

Fig. 6. Contrast-enhanced ultrasound of the PDAC tumour in Patient 7. Panel A: B-mode image. Panel B: Contrast-Enhanced image using SonoVue® microbubbles. Pancreatic tissue, the PDAC tumour and aorta have been labeled. Microbubbles can be clearly distinguished in the PDAC tumour when comparing to the B-Mode image. Panel C: Perfusion curve depicting non-linear echo amplitude as a function of time for the three regions of interest: Aorta (yellow), pancreatic tissue (red) and PDAC tumour (cyan). The PDAC tumour exhibits a longer time-to-peak and lower perfusion than both the aorta and pancreas, yet is still adequately perfused for microbubbles to enter. Panels A and B are freeze frames of late phase perfusion, 57 s after microbubbles injection (*c.f.*, white arrows in Panel C).

tumour progression it does not take into account the 3D structural change of the tumour. In our opinion, future work should address the treatment effect on the tumour volume and not only the maximal diameter.

The primary limitations of this study are that only a single 2D slice of the tumour was treated. Using a 3D ultrasound probe with further optimized acoustic conditions and modifying the microbubble type and concentration may improve the therapeutic efficacy [44].

The ultrasound emission conditions used here were severely limited by the clinical diagnostic scanner. In previous studies, longer duty cycles have shown to have a better therapeutic effect than short duty cycles [76]. Future work should aim to determine the ultrasound conditions that induce the highest therapeutic effect and to allow implementation of such conditions in the clinic.

There is currently no consensus on what is considered an ideal microbubble dose. At high dosages, the microbubbles may interact more with each other than the cells due to secondary Bjerknes forces [42], whereas at low concentrations, there may not be enough microbubbles to interact with the cells. Future work should evaluate and optimise the microbubble type and dosage.

In the field of sonoporation, it is typically assumed that the enhanced effect is due to the increase in local drug concentrations. In our work, we did not evaluate if the local drug concentration was increased and if this could be the reason for the enhanced effect. Future work should evaluate if there is an increase in local drug concentration, or if the improved therapeutic efficacy is due to increase or decrease in perfusion, or other intracellular responses.

5. Conclusion

In conclusion, our study indicated that chemotherapy in combination with ultrasound and microbubbles seems to be safe. No additional toxicity was observed when compared to chemotherapy alone. In our patient cohort, sonoporation has the additional benefit of improving the number of treatment cycles the patients were able to undergo and correspondingly extending the period of well-being. Significantly increased survival was also observed compared to a historical cohort of patients. Acknowledging the small treatment group with sub-optimal treatment conditions in this study, a larger study with improved acoustic conditions and microbubble delivery is essential to improve our understanding and validating our results. Nevertheless, in our opinion these novel results show great promise for ultrasound and microbubble enhanced therapy.

Supplementary data to this article can be found online at http://dx.doi.org/10.1016/j.jconrel.2016.10.007.

Ethical considerations

The protocol was approved by the Regional Ethics Committee (2011/1601/REK vest) and the Norwegian Medicines Agency (NMA). The study was performed in accordance with the Helsinki Declaration. All subjects signed an informed consent.

Conflict of interest disclosure statement

I declare no conflict of interest Georg Dimcevski, Date: 06/10/2016, Bergen Norway.

Acknowledgements

This study has received initial financial support from the Norwegian Cancer Society (11007001), Helse Vest (911779), and MedViz (03-2014) (http://medviz.uib.no/), a research consortium from Haukeland University Hospital, University of Bergen and Christian Michelsen Research AS. We give our special acknowledgement to our chemotherapy administrating oncologists Nils Glenjen and Hämmerling Katrin. And special thanks to our nurses (Hilde Sælensminde, Torill Våge, Marianne Lehmann, Mari Holsen, Elisabeth Bjerkan) at the Clinical Trial Unit at Haukeland University Hospital for taking care of our patients.

References

[1] World Cancer Report. 2014.
[2] A. Neesse, P. Michl, K.K. Frese, C. Feig, N. Cook, M.A. Jacobetz, M.P. Lolkema, M. Buchholz, K.P. Olive, T.M. Gress, D.A. Tuveson, Stromal biology and therapy in pancreatic cancer, Gut 60 (2011) 861–868.
[3] Kreftregisteret, Cancer in Norway, 2010.
[4] N. Alexakis, C. Halloran, M. Raraty, P. Ghaneh, R. Sutton, J.P. Neoptolemos, Current standards of surgery for pancreatic cancer, Br J Surg 91 (2004) 1410–1427.
[5] M. Malvezzi, P. Bertuccio, F. Levi, V.C. La, E. Negri, European cancer mortality predictions for the year 2013, Ann. Oncol. 24 (2013) 792–800.
[6] H.A. Burris III, M.J. Moore, J. Andersen, M.R. Green, M.L. Rothenberg, M.R. Modiano, M.C. Cripps, R.K. Portenoy, A.M. Storniolo, P. Tarassoff, R. Nelson, F.A. Dorr, C.D. Stephens, D.D. Von Hoff, Improvements in survival and clinical benefit with gemcitabine as first-line therapy for patients with advanced pancreas cancer: a randomized trial, J. Clin. Oncol. 15 (1997) 2403–2413.
[7] T. Conroy, C. Gavoille, E. Samalin, M. Ychou, M. Ducreux, The role of the FOLFIRINOX regimen for advanced pancreatic cancer, Curr. Oncol. Rep. 15 (2013) 182–189.
[8] S.M. Hoy, Albumin-bound paclitaxel: a review of its use for the first-line combination treatment of metastatic pancreatic cancer, Drugs 74 (2014) 1757–1768.
[9] B.B. Goldberg, R. Gramiak, A.K. Freimanis, Early history of diagnostic ultrasound: the role of American radiologists, AJR Am. J. Roentgenol. 160 (1993) 189–194.
[10] S. Ødegaard, Gilja OH, Gregersen H, Basic and New Aspects of Gastrointestinal Ultrasonography, 2005.
[11] B.J. Ostrum, B.B. Goldberg, H.J. Isard, A-mode ultrasound differentiation of soft-tissue masses, Radiology 88 (1967) 745–749.
[12] G.A. Zamboni, M.C. Ambrosetti, M. D'Onofrio, M.R. Pozzi, Ultrasonography of the pancreas, Radiol. Clin. N. Am. 50 (2012) 395–406.
[13] Y. Wei, X.L. Yu, P. Liang, Z.G. Cheng, Z.Y. Han, F.Y. Liu, J. Yu, Guiding and controlling percutaneous pancreas biopsies with contrast-enhanced ultrasound: target lesions are not localized on B-mode ultrasound, Ultrasound Med. Biol. 41 (2015) 1561–1569.
[14] D.L. Miller, J. Quddus, Sonoporation of monolayer cells by diagnostic ultrasound activation of contrast-agent gas bodies, Ultrasound Med. Biol. 26 (2000) 661–667.
[15] J. Wu, J.P. Ross, J.F. Chiu, Reparable sonoporation generated by microstreaming, J. Acoust. Soc. Am. 111 (2002) 1460–1464.
[16] S. Bao, B.D. Thrall, D.L. Miller, Transfection of a reporter plasmid into cultured cells by sonoporation in vitro, Ultrasound Med. Biol. 23 (1997) 953–959.
[17] B.H. Lammertink, C. Bos, K.M. van der Wurff-Jacobs, G. Storm, C.T. Moonen, R. Deckers, Increase of intracellular cisplatin levels and radiosensitization by ultrasound in combination with microbubbles, J. Control. Release 238 (2016) 157–165.
[18] M. Derieppe, K. Rojek, J.M. Escoffre, B.D. de Senneville, C. Moonen, C. Bos, Recruitment of endocytosis in sonopermeabilization-mediated drug delivery: a real-time study, Phys. Biol. 12 (2015) 046010.
[19] v. WA, S. PC, A. Healey, S. Kvale, N. Bush, J. Bamber, d.L. DC, Acoustic cluster therapy (ACT) enhances the therapeutic efficacy of paclitaxel and Abraxane(R) for treatment of human prostate adenocarcinoma in mice, J. Control. Release 236 (2016) 15–21.
[20] S. Eggen, S.M. Fagerland, Y. Morch, R. Hansen, K. Sovik, S. Berg, H. Furu, A.D. Bohn, M.B. Lilledahl, A. Angelsen, B. Angelsen, D.C. de Lange, Ultrasound-enhanced drug delivery in prostate cancer xenografts by nanoparticles stabilizing microbubbles, J. Control. Release 187 (2014) 39–49.
[21] I. Lentacker, B. Geers, J. Demeester, S.C. De Smedt, N.N. Sanders, Design and evaluation of doxorubicin-containing microbubbles for ultrasound-triggered doxorubicin delivery: cytotoxicity and mechanisms involved, Mol. Ther. 18 (2010) 101–108.
[22] B. Theek, M. Baues, T. Ojha, D. Mockel, S.K. Veettil, J. Steitz, v. BL, G. Storm, F. Kiessling, T. Lammers, Sonoporation enhances liposome accumulation and penetration in tumors with low EPR, J. Control. Release 231 (2016) 77–85.
[23] M. Bazan-Peregrino, C.D. Arvanitis, B. Rifai, L.W. Seymour, C.C. Coussios, Ultrasound-induced cavitation enhances the delivery and therapeutic efficacy of an oncolytic virus in an in vitro model, J. Control. Release 157 (2012) 235–242.
[24] N. McDannold, C.D. Arvanitis, N. Vykhodtseva, M.S. Livingstone, Temporary disruption of the blood-brain barrier by use of ultrasound and microbubbles: safety and efficacy evaluation in rhesus macaques, Cancer Res. 72 (2012) 3652–3663.
[25] S.M. Fix, M.A. Borden, P.A. Dayton, Therapeutic gas delivery via microbubbles and liposomes, J. Control. Release 209 (2015) 139–149.
[26] F. Prieur, A. Pillon, J.L. Mestas, V. Cartron, P. Cebe, N. Chansard, M. Lafond, C. Lafon, Enhancement of fluorescent probe penetration into tumors in vivo using unseeded inertial cavitation, Ultrasound Med. Biol. 42 (2016) 1706–1713.
[27] I. Lentacker, B. Geers, J. Demeester, S.C. De Smedt, N.N. Sanders, Design and evaluation of doxorubicin-containing microbubbles for ultrasound-triggered doxorubicin delivery: cytotoxicity and mechanisms involved, Mol. Ther. 18 (2010) 101–108.
[28] B.D. de Senneville, C. Moonen, M. Ries, MRI-Guided HIFU methods for the ablation of liver and renal cancers, Adv. Exp. Med. Biol. 880 (2016) 43–63.
[29] Ebbini ES, ter HG. Ultrasound-guided therapeutic focused ultrasound: current status and future directions. Int. J. Hyperth. 2015;31:77–89.
[30] G. Shapiro, A.W. Wong, M. Bez, F. Yang, S. Tam, L. Even, D. Sheyn, S. Ben-David, W. Tawackoli, G. Pelled, K.W. Ferrara, D. Gazit, Multiparameter evaluation of in vivo gene delivery using ultrasound-guided, microbubble-enhanced sonoporation, J. Control. Release 223 (2016) 157–164.

[31] I. De C, G. Lajoinie, M. Versluis, D.S. SC, I. Lentacker, Sonoprinting and the importance of microbubble loading for the ultrasound mediated cellular delivery of nanoparticles, Biomaterials 83 (2016) 294–307.
[32] M. Postema, S. Kotopoulis, A. Delalande, Odd Helge Gilja. Sonoporation: why microbubbles create pores, Ultraschall in Med 2012 33 (1) (2016) 97–98.
[33] v. RT, I. Skachkov, I. Beekers, L. KR, V. JD, K. TJ, D. Bera, Y. Luan, v. der Steen AF, d. JN, K. Kooiman, Viability of endothelial cells after ultrasound-mediated sonoporation: influence of targeting, oscillation, and displacement of microbubbles, J. Control. Release 238 (2016) 197–211.
[34] A. Delalande, C. Leduc, P. Midoux, M. Postema, C. Pichon, Efficient gene delivery by sonoporation is associated with microbubble entry into cells and the clathrin-dependent endocytosis pathway, Ultrasound Med. Biol. 41 (2015) 1913–1926.
[35] M. Chan, K. Dennis, Y. Huang, C. Mougenot, E. Chow, C. DeAngelis, J. Coccagna, A. Sahgal, K. Hynynen, G. Czarnota, W. Chu, Magnetic resonance-guided high-intensity-focused ultrasound for palliation of painful skeletal metastases: a pilot study, Technol Cancer Res Treat (2016).
[36] A. Waspe, Y. Huang, R. Endre, J. Amaral, J. de Ruiter, F. Campbell, C. Mougenot, K. Hynynen, G. Czarnota, J. Drake, M. Temple, Magnetic resonance guided focused ultrasound for noninvasive pain therapy of osteoid osteoma in children, Journal of Therapeutic Ultrasound 3 (Suppl 1) (2015) O48 2015.
[37] K. Hynynen, O. Pomeroy, D.N. Smith, P.E. Huber, N.J. McDannold, J. Kettenbach, J. Baum, S. Singer, F.A. Jolesz, MR imaging-guided focused ultrasound surgery of fibroadenomas in the breast: a feasibility study, Radiology 219 (2001) 176–185.
[38] A. Carpentier, M. Canney, A. Vignot, V. Reina, K. Beccaria, C. Horodyckid, C. Karachi, D. Leclercq, C. Lafon, J.Y. Chapelon, L. Capelle, P. Cornu, M. Sanson, K. Hoang-Xuan, J.Y. Delattre, A. Idbaih, Clinical trial of blood-brain barrier disruption by pulsed ultrasound, Sci. Transl. Med. 8 (2016) 343re2.
[39] M. Anzidei, B.C. Marincola, M. Bezzi, G. Brachetti, F. Nudo, E. Cortesi, P. Berloco, C. Catalano, A. Napoli, Magnetic resonance-guided high-intensity focused ultrasound treatment of locally advanced pancreatic adenocarcinoma: preliminary experience for pain palliation and local tumor control, Investig. Radiol. 49 (2014) 759–765.
[40] A. Delalande, S. Kotopoulis, T. Rovers, C. Pichon, M. Postema, Sonoporation at a low mechanical index, Bubble Science, Engineering & Technology 3 (2011) 3–12.
[41] A. Delalande, S. Kotopoulis, M. Postema, P. Midoux, C. Pichon, Sonoporation: mechanistic insights and ongoing challenges for gene transfer, Gene 525 (2013) 191–199.
[42] S. Kotopoulis, M. Postema, Microfoam formation in a capillary, Ultrasonics 50 (2010) 260–268.
[43] S. Kotopoulis, G. Dimcevski, O.H. Gilja, D. Hoem, M. Postema, Treatment of human pancreatic cancer using combined ultrasound, microbubbles, and gemcitabine: a clinical case study, Med. Phys. 40 (2013) 072902.
[44] S. Kotopoulis, A. Delalande, M. Popa, V. Mamaeva, G. Dimcevski, O.H. Gilja, M. Postema, B.T. Gjertsen, E. McCormack, Sonoporation-enhanced chemotherapy significantly reduces primary tumour burden in an orthotopic pancreatic cancer xenograft, Mol. Imaging Biol. 16 (2014) 53–62.
[45] Highlights of Prescribing Information: Gemzar, Eli Lilly and Company, Indianapolis, Indiana, 2010.
[46] M.M. Oken, R.H. Creech, D.C. Tormey, J. Horton, T.E. Davis, E.T. McFadden, P.P. Carbone, Toxicity and response criteria of the eastern cooperative oncology group, Am. J. Clin. Oncol. 5 (1982) 649–655.
[47] European Medicines Agency, Guideline for good clinical practice, ICH Topic E 6 (R1) (2002).
[48] L.S. Tham, L.Z. Wang, R.A. Soo, H.S. Lee, S.C. Lee, B.C. Goh, N.H. Holford, Does saturable formation of gemcitabine triphosphate occur in patients? Cancer Chemother. Pharmacol. 63 (2008) 55–64.
[49] M. Schneider, Characteristics of SonoVue®, Echocardiography 16 (1999) 743–746.
[50] S. Schafer, K. Nylund, F. Saevik, T. Engjom, M. Mezl, R. Jirik, G. Dimcevski, O.H. Gilja, K. Tonnies, Semi-automatic motion compensation of contrast-enhanced ultrasound images from abdominal organs for perfusion analysis, Comput. Biol. Med. 63 (2015) 229–237.
[51] F. Piscaglia, C. Nolsoe, D. CF, C. DO, G. OH, B. NM, T. Albrecht, L. Barozzi, M. Bertolotto, O. Catalano, M. Claudon, C. DA, C. JM, M. D'Onofrio, D. FM, J. Eyding, M. Giovannini, M. Hocke, A. Ignee, J. EM, K. AS, N. Lassau, E. Leen, G. Mathis, A. Saftoiu, G. Seidel, S. PS, H. GT, D. Timmerman, W. HP, The EFSUMB Guidelines and Recommendations on the Clinical Practice of Contrast Enhanced Ultrasound (CEUS): update 2011 on non-hepatic applications, Ultraschall Med. (2011).
[52] M. Claudon, D. Cosgrove, T. Albrecht, L. Bolondi, M. Bosio, F. Calliada, J.M. Correas, K. Darge, C. Dietrich, M. D'Onofrio, D.H. Evans, C. Filice, L. Greiner, K. Jager, N. Jong, E. Leen, R. Lencioni, D. Lindsell, A. Martegani, S. Meairs, C. Nolsoe, F. Piscaglia, P. Ricci, G. Seidel, B. Skjoldbye, L. Solbiati, L. Thorelius, F. Tranquart, H.P. Weskott, T. Whittingham, Guidelines and good clinical practice recommendations for contrast enhanced ultrasound (CEUS) - update 2008, Ultraschall Med. 29 (2008) 28–44.
[53] U.S. Department of Health and Human Services, Information for Manufacturers Seeking Marketing Clearance of Diagnostic Ultrasound Systems and Transducers (Food and Drug Administration), 2008.
[54] International Electrotechnical Commission, Ultrasonics - Hydrophones Part 2: Calibration for Ultrasonic Fields up to 40 MHz, Report No. 62127-2 ed1.0, IEC, Geneva, Switzerland, 2013.
[55] d. JN, M. Emmer, v. WA, M. Versluis, Ultrasonic characterization of ultrasound contrast agents, Med. Biol. Eng. Comput. 47 (2009) 861–873.
[56] G. Dimcevski, F.G. Erchinger, R. Havre, O.H. Gilja, Ultrasonography in diagnosing chronic pancreatitis: new aspects, World J. Gastroenterol. 19 (2013) 7247–7257.
[57] F. Erchinger, G. Dimcevski, T. Engjom, O.H. Gilja, Transabdominal ultrasound of the pancreas: basic and new aspects, Imaging in Medicine 3 (2011) 411–422.
[58] T. Bjanes, T. Kamceva, T. Eide, B. Riedel, J. Schjott, A. Svardal, Preanalytical stability of gemcitabine and its metabolite 2′, 2′-difluoro-2′-deoxyuridine in whole blood-assessed by liquid chromatography tandem mass spectrometry, J. Pharm. Sci. (2015).
[59] S.A. Sohaib, B. Turner, J.A. Hanson, M. Farquharson, R.T. Oliver, R.H. Reznek, CT assessment of tumour response to treatment: comparison of linear, cross-sectional and volumetric measures of tumour size, Br. J. Radiol. 73 (2000) 1178–1184.
[60] C.P. Nolsoe, T. Lorentzen, International guidelines for contrast-enhanced ultrasonography: ultrasound imaging in the new millennium, Ultrasonography 35 (2016) 89–103.
[61] R.L. Wahl, H. Jacene, Y. Kasamon, M.A. Lodge, From RECIST to PERCIST: evolving considerations for PET response criteria in solid tumors, J. Nucl. Med. 50 (Suppl 1) (2009) 122S–150S.
[62] J.L. Abbruzzese, R. Grunewald, E.A. Weeks, D. Gravel, T. Adams, B. Nowak, S. Mineishi, P. Tarassoff, W. Satterlee, M.N. Raber, A phase I clinical, plasma, and cellular pharmacology study of gemcitabine, J. Clin. Oncol. 9 (1991) 491–498.
[63] H. Inoue, Y. Arai, T. Kishida, M. Shin-Ya, R. Terauchi, S. Nakagawa, M. Saito, S. Tsuchida, A. Inoue, T. Shirai, H. Fujiwara, O. Mazda, T. Kubo, Sonoporation-mediated transduction of siRNA ameliorated experimental arthritis using 3 MHz pulsed ultrasound, Ultrasonics 54 (2014) 874–881.
[64] H. Dewitte, L.S. Van, C. Heirman, K. Thielemans, S.C. De Smedt, K. Breckpot, I. Lentacker, The potential of antigen and TriMix sonoporation using mRNA-loaded microbubbles for ultrasound-triggered cancer immunotherapy, J. Control. Release 194 (2014) 28–36.
[65] I. Skachkov, Y. Luan, A.F. van der Steen, d. JN, K. Kooiman, Targeted microbubble mediated sonoporation of endothelial cells in vivo, IEEE Trans. Ultrason. Ferroelectr. Freq. Control 61 (2014) 1661–1667.
[66] A.H. Ko, J. Hwang, A.P. Venook, J.L. Abbruzzese, E.K. Bergsland, M.A. Tempero, Serum CA19-9 response as a surrogate for clinical outcome in patients receiving fixed-dose rate gemcitabine for advanced pancreatic cancer, Br. J. Cancer 93 (2005) 195–199.
[67] A. Vincent, J. Herman, R. Schulick, R.H. Hruban, M. Goggins, Pancreatic cancer, Lancet 378 (2011) 607–620.
[68] N. Makrilia, K.N. Syrigos, M.W. Saif, Updates on treatment of gemcitabine-refractory pancreatic adenocarcinoma. Highlights from the "2011 ASCO annual meeting". Chicago, IL, USA; June 3-7, 2011, JOP 12 (2011) 351–354.
[69] P.F. Peddi, S. Lubner, R. McWilliams, B.R. Tan, J. Picus, S.M. Sorscher, R. Suresh, A.C. Lockhart, J. Wang, C. Menias, F. Gao, D. Linehan, A. Wang-Gillam, Multi-institutional experience with FOLFIRINOX in pancreatic adenocarcinoma, JOP 13 (2012) 497–501.
[70] A. Neesse, S. Krug, T.M. Gress, D.A. Tuveson, P. Michl, Emerging concepts in pancreatic cancer medicine: targeting the tumor stroma, Onco Targets Ther 7 (2013) 33–43.
[71] C. Bosetti, P. Bertuccio, M. Malvezzi, F. Levi, L. Chatenoud, E. Negri, V.C. La, Cancer mortality in Europe, 2005-2009, and an overview of trends since 1980, Ann. Oncol. 24 (2013) 2657–2671.
[72] A. Bouakaz, A. Zeghimi, A.A. Doinikov, Sonoporation: concept and mechanisms, Adv. Exp. Med. Biol. 880 (2016) 175–189.
[73] B. Helfield, X. Chen, S.C. Watkins, F.S. Villanueva, Biophysical insight into mechanisms of sonoporation, Proc. Natl. Acad. Sci. U. S. A. 113 (2016) 9983–9988.
[74] F. Yuan, M. Dellian, D. Fukumura, M. Leunig, D.A. Berk, V.P. Torchilin, R.K. Jain, Vascular permeability in a human tumor xenograft: molecular size dependence and cutoff size, Cancer Res. 55 (1995) 3752–3756.
[75] S. Kotopoulis, R. Haugsez, M. Mujic, A. Sulen, S.E. Gullaksen, E. McCormack, O.H. Gilja, M. Postema, B.T. Gjertsen, Evaluation of the effects of clinical diagnostic ultrasound in combination with ultrasound contrast agents on cell stress: Single cell analysis of intracellular phospho-signaling pathways in blood cancer cells and normal blood leukocytes. Ultrasonics Symposium (IUS), IEEE International (3–6 Sept. 2014).
[76] P. Reuter, J. Masomi, H. Kuntze, I. Fischer, K. Helling, C. Sommer, B. Alessandri, A. Heimann, T. Gerriets, J. Marx, O. Kempski, M. Nedelmann, Low-frequency therapeutic ultrasound with varied duty cycle: effects on the ischemic brain and the inner ear, Ultrasound Med. Biol. 36 (2010) 1188–1195.